

Terra/MODIS and Aqua/MODIS Normalized Water-Leaving Radiance Algorithm Enhancements and Tests

Kenneth Voss, Howard Gordon, and Nordine Souaidia
Physics Department, University of Miami

MODIS Instrument Polarization: Ray Trace Modeling with David Moyer[SSAI], Gerhard Meister[GSFC/NASA], Sam Pellicori[Pellicore Optical Consulting], Eugene Waluschka [GSFC/NASA]

Introduction

Both MODIS instruments (Aqua and Terra) were fully characterized and calibrated prior to the launch. The polarization sensitivity of MODIS was characterized by Santa Barbara Remote Sensing (SBRS) using a linearly polarized source (the PSA) as input. Once the system is on orbit, there is no way to measure the polarization sensitivity changes that have occurred on orbit other than through their effects on the retrieved products. We started a program to try to produce a polarization ray tracing simulation of the MODIS instrument which could then be used to study the effect of degradation of the instrument optical coatings on the polarization sensitivity of the MODIS instrument.

The polarization data obtained by SBRS was used to check the results of our polarization ray tracing analysis. In order to perform our simulation, the full geometrical specifications of MODIS were necessary along with all coatings prescriptions. The MODIS optical system data was provided by NASA GSFC. The coating characteristics though could not be obtained from the manufacturer. Thus reverse engineering was employed in order to retrieve the characteristics of each coating. Our model simulation was performed using the ZEMAX Optical Ray Tracing software.

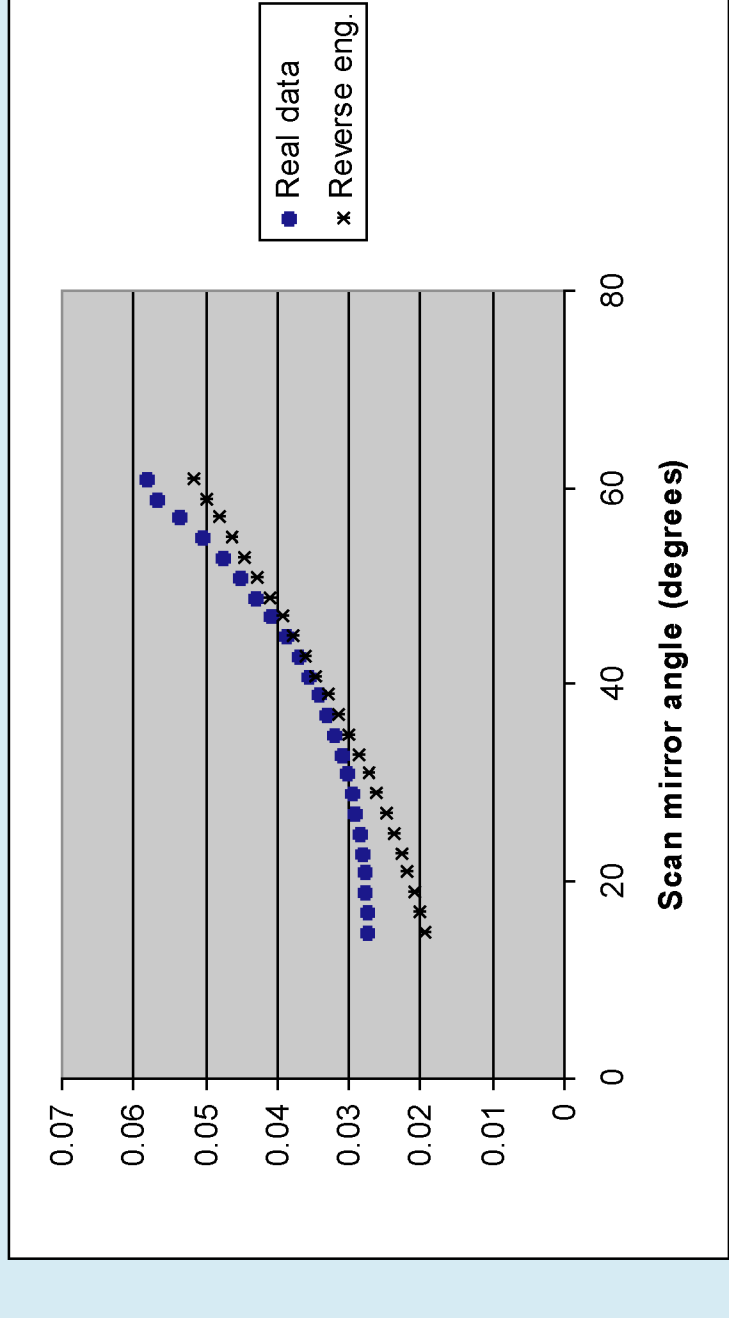
MODIS optical system in ZEMAX

The full geometrical specifications of MODIS were provided by NASA in the form of a ZEMAX lens file. This file contains data for each optical element of the system. MODIS consists of 3 types of optical elements: Mirrors, Beam splitters and Lenses. Since the coating data could not be provided by the manufacturer, reverse engineering was used to retrieve the optical properties of each coating available in MODIS. This work was performed by Pellicori Optical Consulting (POC) based on Transmission and Reflection tables from the pre-launch characterization. A preliminary analysis of the MODIS optical system showed which that the scan mirror and 2 dichroic beam splitters coatings were critical for the polarization analysis. Thus efforts were made to get a best match for these coating. Other optical elements had rays going through with small angle of incidence (AOI) which had little effect on the polarization.

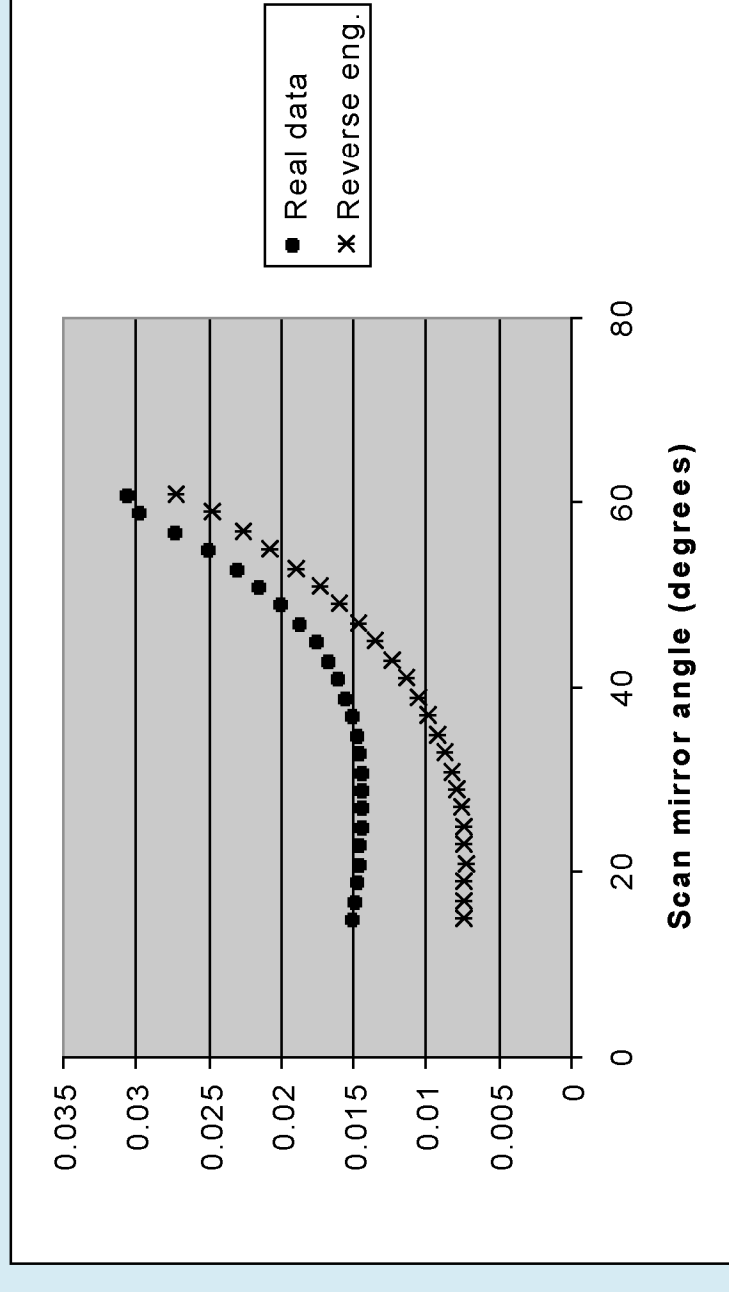
Polarization sensitivity analysis in ZEMAX

The polarization sensitivity analysis was performed at Santa Barbara Remote Sensing (SBRS) using a linearly polarized light source as input to the MODIS optical system. This source was rotated from 0 to 180 degrees and MODIS data was recorded. This was repeated for several angles of the scan mirror ranging between 15.5 and 60.5 degrees angle of incidence (AOI). In ZEMAX we virtually reproduced this experiment with the use of a ZPL (ZEMAX Programming Language) macro. A bundle of ray filling the entrance aperture was sent through the optical system at wavelengths within the range of each MODIS filter. In order to better simulate the SBRS experiment, the data was then pupil and wavelength averaged. This was repeated for various combinations of polarization angle and scan mirror angle. We obtained plots of the transmitted signal vs. polarization angle for each scan mirror angle computed.

We had both the reverse engineering coatings and Rs and Rp measurements of the individual surfaces. Since ZEMAX allows the use of both coating values and use of specific Rs and Rp values, we ran the simulation both ways. The results were compared to the SBRS data.



MODIS Band 8 polarization amplitude results. Real data is ray trace simulation based on Rs and Rp measurements of each surface. Reverse Engineering result is based on the coating thicknesses and types that had to be estimated.



MODIS Band 9 polarization amplitude results. Similar to figure to left.

The MODIS optical system transmittance was computed for various combinations of polarization angle and scan mirror angle. For every scan angle we obtained a table of the transmittance vs. polarization angle. The data was fitted to the following equation to retrieve the polarization sensitivity parameters:

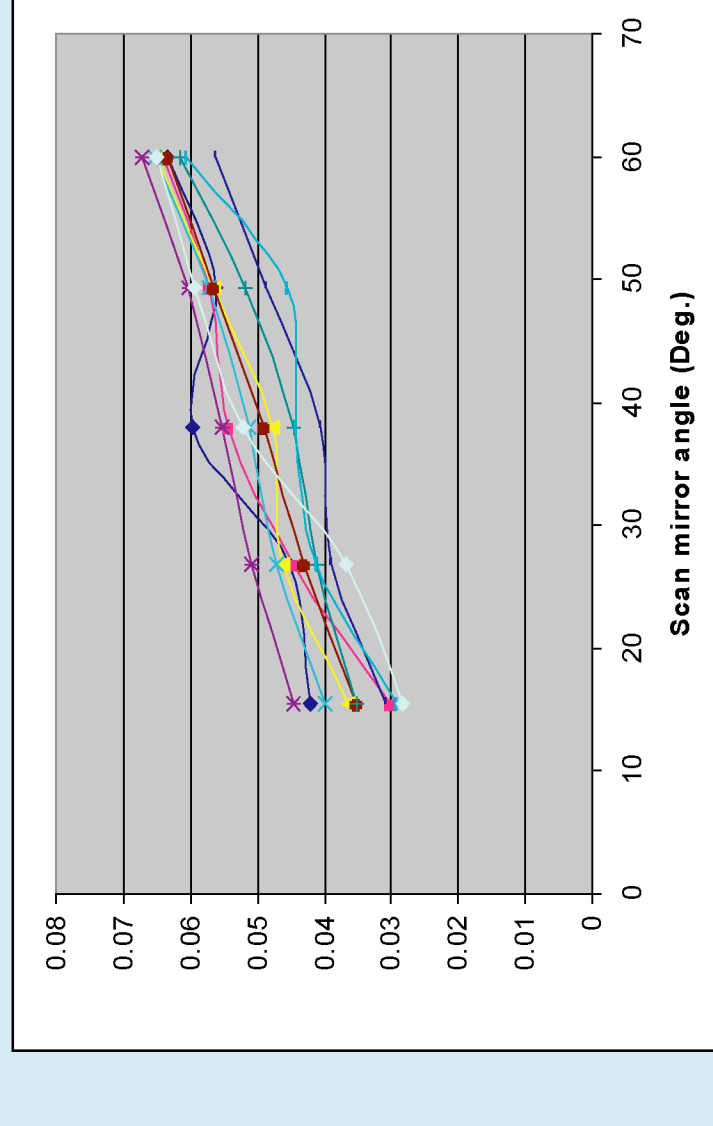
$$T = A(1 + \alpha \cdot \cos(2\theta + \phi))$$

Where:
T is the transmitted signal through the MODIS optical system.
A is the average transmitted signal.
 α is the polarization amplitude.
 θ is the polarization angle.
 ϕ is the phase angle.

The SBRS pre-launch polarization analysis showed that the polarization amplitude was higher for Band 8 and 9 (412nm and 453nm) compared to other bands. We thus optimized the reverse engineering process that computed the coatings data for the 400 to 500nm region of the spectrum.

As can be seen above, the Band 8 simulated coating prescription gave approximately the same results as the measured coating prescriptions. For Band 9, we noticed a difference but the overall behavior was similar. For the remainder of the work, we concentrated our efforts on Band 8, since this Band 8 had the largest polarization effect.

Prior to the MODIS launch, SBRS performed a polarization sensitivity analysis on the optical system, including for each detector. When we analyzed our results for each detector we got the following:



SBRS pre-launch polarization measurements of all detectors for Band 8 (Based on reverse engineered coatings)

The results show a good agreement between pre-launch (SBRS) and simulated (ZEMAX) data for band 8. Simulated data are in general lower than measured data. Uncertainties for this simulation can come from various sources. The reverse engineered coating design is a first source of uncertainty though we have seen that the simulated coating optical properties match with the real coating properties. Uncertainties in the pre-launch SBRS data also affect the comparison. As can be seen, the model does not predict significant difference between detectors. It is possible the spread in measurements is indicative of the error in these measurements.

BRDF Influence on the Diffuse Transmittance

The water-leaving radiance is related to the top of the atmosphere radiance by:

$$L_{toa} = (L_r + L_a + L_g) \cdot t_{d,w}$$

For ocean color the desired quantity is L_w and atmospheric correction is the process of determining the quantities L_r (Rayleigh radiance), L_a (aerosol path radiance) and L_g (surface glitter, whitecaps, etc) to obtain $t_{d,w}$.

To date the diffuse transmittance (t) has been calculated, using information determined from the aerosol derived in the atmospheric correction process, but ignoring directional effects of the angular distribution of the upwelling radiance field. The current operational assumption is that the upwelling sub-surface radiance distribution is uniform.

In recent years we have been making measurements of the upwelling radiance distribution, and this experimental work, combined with the modeling work of others (Morel, Gentili, and others, 1993-2002) have shown that the uniform upwelling radiance distribution is not uniform, and the variation must be taken into account (the so-called BRDF effect).

Just as the variations in the BRDF must be taken into account when looking at L_w , ignoring the BRDF when calculating t can lead to errors in L_w of several percent (Yang and Gordon, 1997). When the proper BRDF is included in the problem, the diffuse transmittance becomes dependent on the direction of the solar beam, the direction of viewing, the aerosol optical thickness and type (e.g., aerosol model) and water optical properties (characterized in the Morel and Gentili model by the concentration of Chlorophyll a (C)).

As an example we show the following figure that illustrates both the error in assuming a uniform BRDF as opposed to real situation (referred to as Exact) and a possible correction.

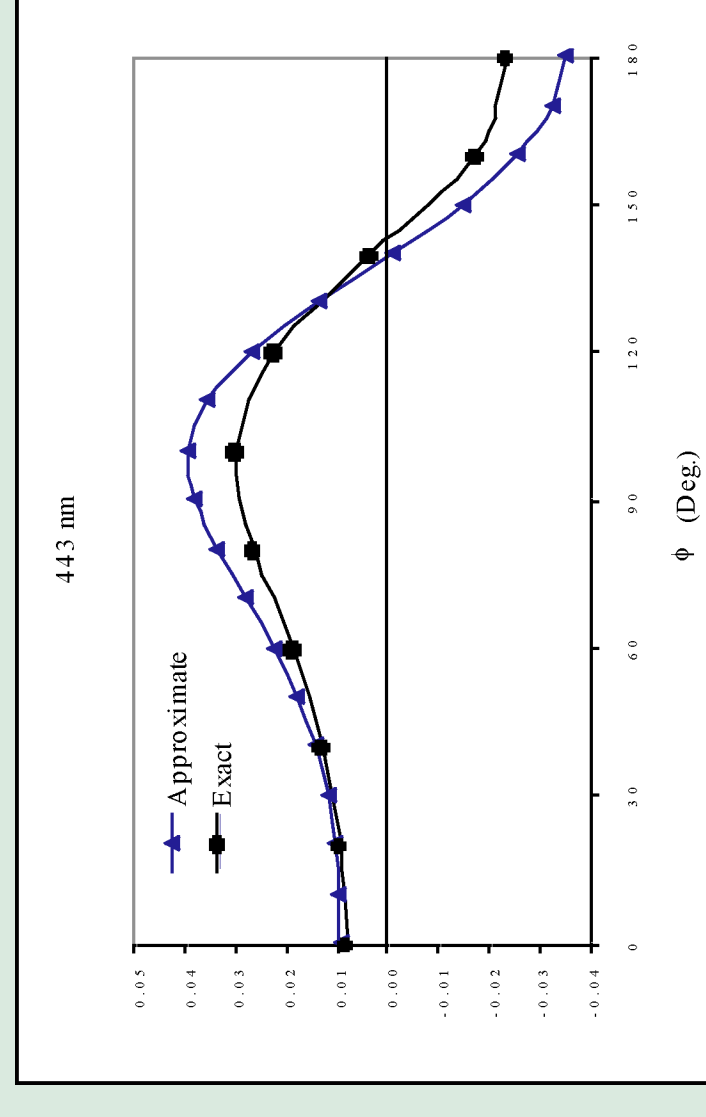


Figure 1. This is the relative difference between the true diffuse transmittance t (including BRDF effects) and the diffuse transmittance t^* , which is computed assuming that the BRDF is uniform. The solar zenith angle is 40 deg. and the viewing zenith angle is 40 deg. The x-axis is the relative azimuth between the solar and viewing directions. The curve labeled "Exact" is the result of complete radiative transfer computations taken from Figure 4C in Gordon and Yang (1997). The curve labeled "Approximate" is the result of the approximate computation described in the text. The aerosol model is M90 and the aerosol optical depth at 443 nm is 0.20.

The dependence of the diffuse transmittance on the BRDF model and on the chlorophyll concentration makes the preparation of look up tables (LUTs) difficult, both because of the added variable and because of the fact that the existing BRDF model is not yet definitive.

Thus, we have been developing an approximate theory of the diffuse transmittance that will allow its computation without the preparation of extensive LUTs. An example of the efficacy of this approach is provided in the Figure above. This compares exact computations taken from Yang and Gordon (their Figure 4C) with the approximate computations (note that the relative azimuth in Gordon and Yang is 180 deg. minus the relative azimuth in Figure 4). Although there is some residual difference between the two results, it is clear that the approximate computation captures the major variability, and is superior to the uniform-BRDF approximation. The prototype software for inclusion of this approximate computation of t into the ocean color processing system is being developed now, and we expect to have it in a form for delivery to GSFC in the spring.

To demonstrate the dependence of the diffuse transmittance on the chlorophyll concentration, we use the Morel and Gentili model of f/Q (Morel et al., 2002) to provide the BRDF as a function of C. Figure 5 provides the f/Q for low and high chlorophyll concentrations and Figure 6 shows that the resulting error made in replacing t by t^* depends significantly on the chlorophyll concentration.

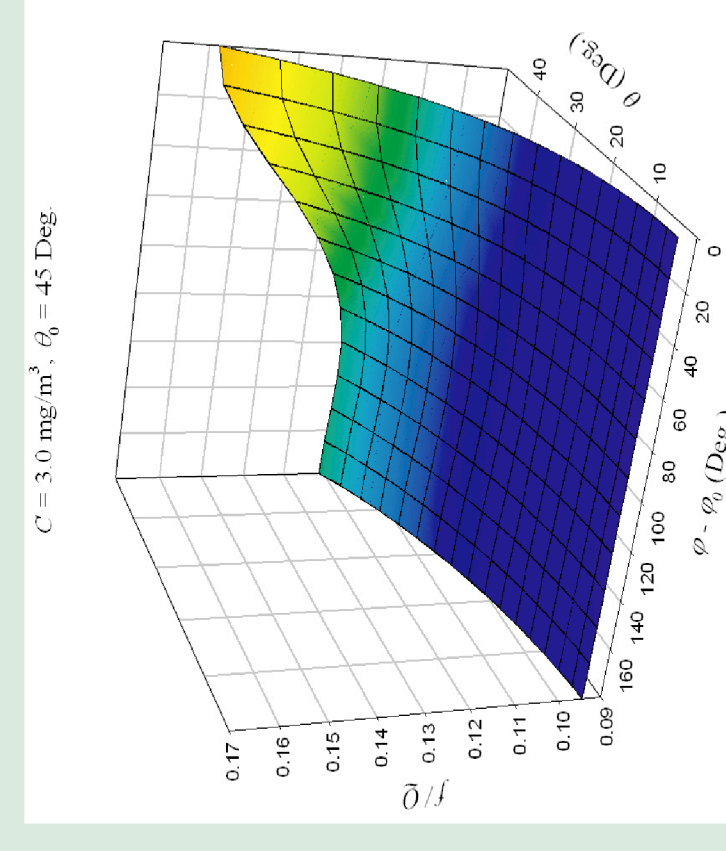
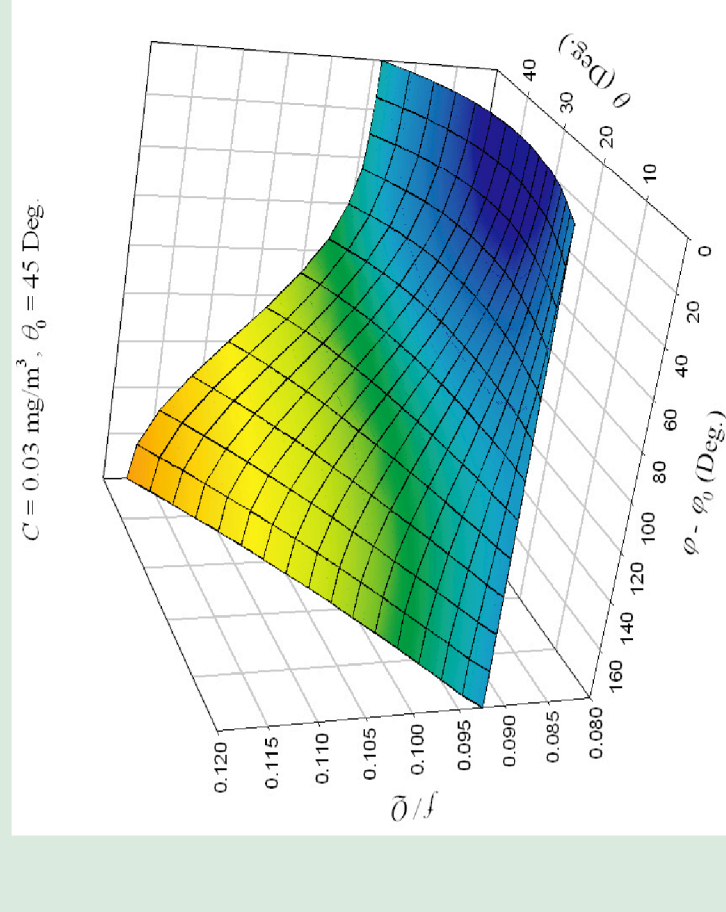


Figure 2: Morel and Gentili-modeled f/Q as a function of viewing direction for low (left) and high (right) chlorophyll concentrations.

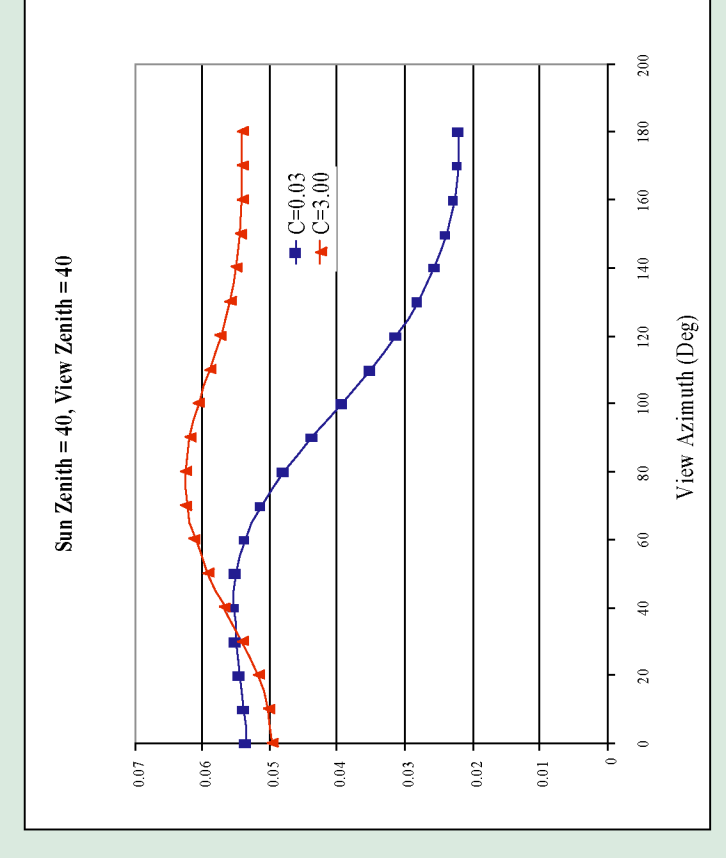


Figure 3: Relative error in using t^* as an approximation to the true diffuse transmittance t for the BRDFs provided in Figure 2. Note that this error results in a similar error in the recovery of the water-

H. Yang and H.R. Gordon, Remote sensing of ocean color: Assessment of the water-leaving radiance bidirectional effects on the atmospheric diffuse transmittance, Applied Optics, 36, 7887-7897 (1997).

A. Morel, D. Antoine and B. Gentili, Bidirectional reflectance of oceanic waters: accounting for Raman emission and varying particle scattering phase function, Applied Optics 41, 6289-6306 (2002).

Polarization in the upwelling water leaving radiance

As part of our work to understand the polarization sensitivity of MODIS, the effects of this polarization on the water leaving radiance, and atmospheric correction algorithm enhancements to adapt to this polarization sensitivity, we are making measurements of the polarized upwelling spectral radiance distribution.

To do this work with our NURADS radiance distribution camera system. This camera system uses a fisheye lens to image the upwelling radiance distribution through spectral filters onto a CCD array camera (Voss and Chapin, 2005). We have three copies of this instrument, and have been using the instrument to investigate the variation in the upwelling radiance distribution (BRDF effect) in various water types.

To describe the polarization state of a partially polarized radiance, we use the Stokes vector representation. This vector is represented as (I, Q, U, V) where I is the total intensity (radiance in this case), Q is the radiance linearly polarized in some reference plane (typically the plane that contains the zenith, or nadir, and the view direction) minus the radiance linearly polarized perpendicular to this direction, U is the radiance polarized in a plane 45 degrees to the Q plane minus the radiance polarized 90 degrees to this plane, and finally V is the right circularly polarized light minus the left circularly polarized light. From the Stokes vector, many other properties can be calculated such as the degree of polarization, plane of polarization, etc.

Previously we have made measurements of the sky polarization components using combinations of images, where a linear polarizer is rotated into 3 different orientations (Voss and Liu, 1997; Liu and Voss, 1997). Because the upwelling radiance distribution is much more dynamic, the images must be taken simultaneously. To do this we have taken our three NURADS systems, and placed them together in an array. The camera electronics and control system were modified to allow simultaneous image capture in the three systems. The pictures below show the instrument in the field during its first sea trials, during early December. We used a MOBY maintenance cruise to provide the opportunity for the test, the pictures show the instrument configuration and deployment strategy.



This picture shows the system on deck. The three separate camera systems image through the glass ports on the bottom of each

canister. Each system has its own cable coming to the surface, and the whole system is supported by the floats as shown.

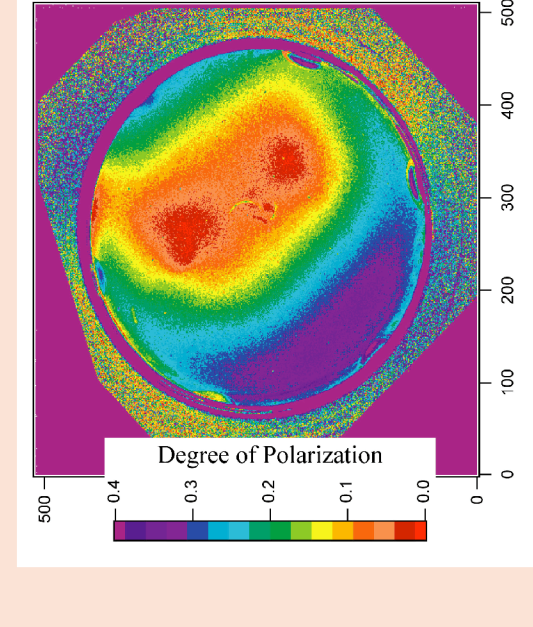


This picture shows the system as it is deployed off the stern of the ship.

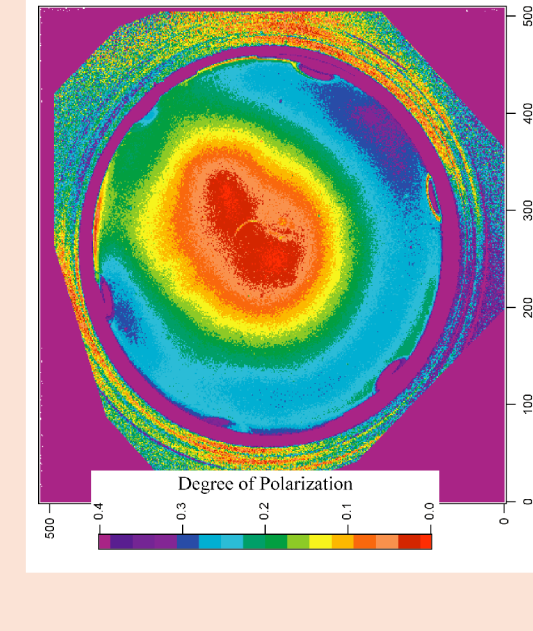
To avoid ship shadowing effects as much as possible, the instrument is allowed to float away from the ship. On this cruise the instrument was approximately 20 m from the ship, we usually have the instrument 50 m or more from the ship.

Example Degree of Polarization images of the upwelling radiance distribution, in clear water, on an overcast day.

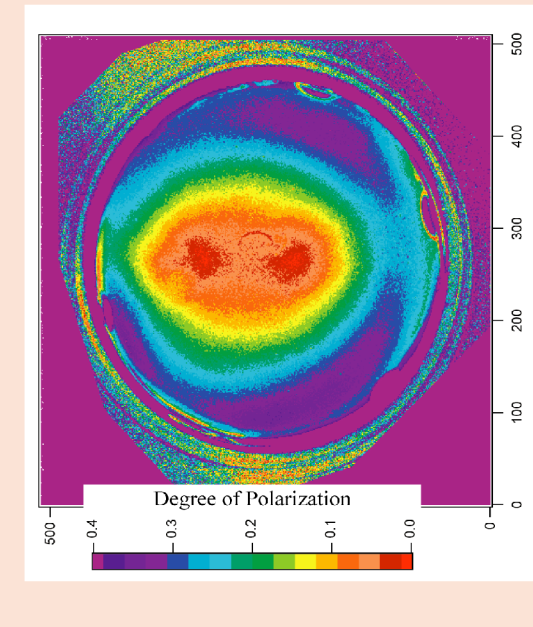
412 nm



488 nm



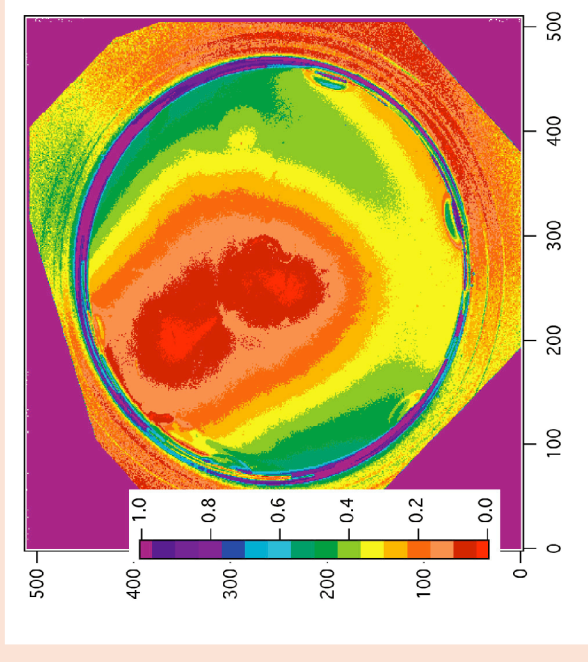
548 nm



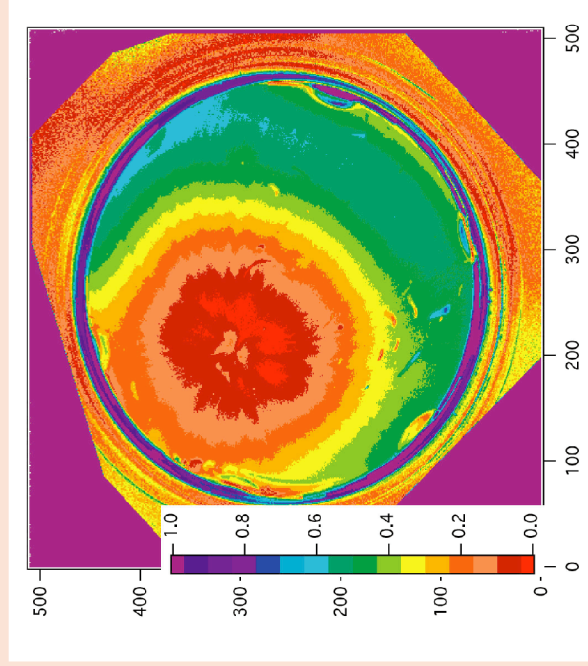
Overcast Sky conditions. The geometry of these image is set so that nadir is in the center of the image. The purple edge of the image is the horizon. Because of surface refraction, the important region for remote sensing is from the center to about halfway out to the horizon. In this region, for overcast conditions, the degree of linear polarization is relatively small.

Example Degree of Polarization images of the upwelling radiance distribution, in clear water, on a clear day.

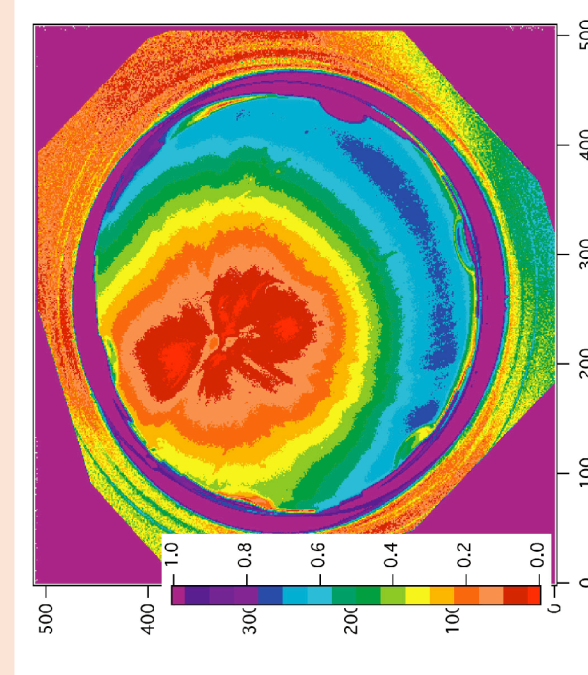
412 nm



488 nm



548 nm



In this clear sky case, the sun angle is 43 degree zenith angle. Note the change in scale, in this case there is much more polarization in the center part of the image. The minimum polarization area is around the anti solar point. At lower sun angles, the maximum in polarization moves closer to nadir, and can be quite large, and spectrally dependent.

These is a very preliminary data reduction of data which were acquired in early Dec. What it shows is that polarization in the upwelling field can be significant, and is dependent on view direction and illumination conditions.

Y. Liu and K. J. Voss, "Polarized radiance distribution measurements of skylight: II. experiment and data", 1997, Applied Optics, 36: 8753 - 8764.

Voss, K. J. and A. L. Chapin, Upwelling radiance distribution camera system, NURADS, Optics Express, 2005, 13 - 4250 - 4262.

K. J. Voss and Y. Liu, "Polarized radiance distribution measurements of skylight: I. system description and characterization", 1997, Applied Optics, 36 - 6083-6094.